# Novel Facile Technique for Synthesis of Stable Cuprous Oxide (Cu₂O) Nanoparticles – an Ageing Effect

Sachin S. Sawant[1,2], Ashok D. Bhagwat[1,3], Chandrashekhar M. Mahajan[2]

[1] *Singhania University, Pacheri Bari, Jhunjhunu – 333515 Rajasthan, India*
[2] *Department of Engineering Sciences and Humanities, Vishwakarma Institute of Technology, Pune – 411037 Maharashtra, India*
[3] *Dnyanshree Institute of Engineering and Technology, Satara – 415013 Maharashtra, India*

A novel facile method to synthesize stable phase of Cuprous Oxide (Cu₂O) nanoparticles at room temperature is demonstrated. The structural and optical properties of (Cu₂O) nanoparticles were investigated by using X-ray diffraction (XRD), UV-VIS Spectroscopy. XRD analysis has indexed nanocrystalline nature of cubical phase Cu₂O with an average edge length of about 20 nm. The Scanning Electron Microscopy (SEM) measurements also ascertain the cubical morphology. The Fourier Transform Infrared Spectroscopy (FTIR) affirms the presence of characteristic functional group of Cu₂O. The absorbance peak at 485 nm in UV-VIS spectra also confirms the Cu₂O synthesis. Furthermore, UV-VIS absorbance spectra at different ageing time substantiate the phase stability of Cu₂O nanoparticles. The ageing leads to blue shift of absorbance peak mainly due to decrease in Cu₂O particle size with no additional absorbance peak in UV-VIS spectra indicating the formation of secondary phase. The reduction in particle size may be attributed to tiny conversion Cu₂O to CuO. The energy band gap measurements from Tauc plots for Cu₂O nanoparticles shows the increasing trend (2.5 eV to 2.8 eV) with ageing time (2 months), owing to quantum confinement effects.

**Keywords:** Aging effect, Bandgap, Cuprous oxide, Nanoparticles, Stability.

## 1. INTRODUCTION

The oxides of different transition metals such as copper, iron, nickel, cobalt, and zinc with nanometer sizes are considered to be prolific for scientific and technological applications. Amongst the transition metal oxides, Cuprous Oxide (Cu₂O) is an important material with unique semiconducting and optical properties. Basically, it is a *p*-type semiconductor with theoretical direct band gap of 2.2 eV [1-6]. Cu₂O has attained significant research interest recently and has emerged as one of the promising candidates for photovoltaic energy conversion due to its high theoretical solar cell efficiency approximately 18 % [7]. In addition to this, it is used in applications such as: photo catalysis [8] Lithium ion batteries [9], optoelectronic and gas sensors [10, 11].

In view of the technological applications, the repeatability, simplicity, safety, high throughput, energy efficiency and low cost of synthesis are the important concerns for the synthesis of nanocrystalline Cu₂O. There are several methods already reported to synthesize Cu₂O nanoparticles. Some of these methods [12-14] make use of either flammable or corrosive reducing agents, costly toxic organic reactants. Some demands significant energy and high temperature reaction environment [15] templates [16] more time [17]. This work reports simple, safe, economical and easy to scale up method to synthesize stable Cu₂O nanoparticles. Furthermore, the key issue of Cu₂O phase stability was also investigated as a function of ageing time.

## 2. EXPERIMENTAL

### 2.1 Materials

AR grade chemical reagents were used for synthesis of Cu₂O nanoparticles. Typically, Copper Sulphate pentahydrate (CuSO₄,5H₂O), Sodium Hydroxide (NaOH), L-Ascorbic Acid (C₆H₈O₆), Polyvinylpyrrolidone (PVP) (K30, Molecular weight 60,000) were purchased from Loba Chemie Pvt. Ltd. Mumbai, Maharashtra, India and were used without further purification.

### 2.2 Method

Typically, 0.398 g of Copper Sulphate pentahydrate (CuSO₄,5H₂O), 0.12 g of Sodium Hydroxide (NaOH) and 0.435 g of L-Ascorbic Acid (C₆H₈O₆) were first dissolved in 20 ml of double distilled water in three separate beakers. Furthermore 0.06 g, Polyvinylpyrrolidone (PVP) was dissolved in 10 ml of double distilled water. Then 6ml of PVP solution was added to 20 ml of Copper Sulphate solution. This was simultaneously added with each of 20 ml of Sodium Hydroxide and Ascorbic Acid solutions. This resulted in formation of yellow-orange colored precipitate of Cu₂O nanoparticles. The precipitate was filtered and then washed several times by double distilled water and dried in an oven (60 °C) to remove water content for 12 hrs and a fine powder of yellow-orange colored Cu₂O nanoparticles was obtained. Fig. 1 depicts photographic illustration of different steps involved in the synthesis of Cu₂O nanoparticles

### 2.3 Characterization

Powder X-ray diffraction pattern (XRD) of Cu₂O nanoparticles was recorded using a (Bruker D-8, Billerica, MA) advance diffractometer with Cu Kα ($\lambda = 1.5406$ Å) as a radiation source, operated at 40 kV and 30 mA with a scan rate of 0.02°/s over the range of 10°-80°. XRD analysis was done to identify the crystalline

phase, structure and to estimate average grain size. The morphological images of samples were obtained by using Scanning Electron Microscope (JOEL, FE-SEM 7000). FTIR analysis was done in the range 4000-400 cm$^{-1}$ with FTIR spectrophotometer (Perkin Elmer Spectrum BX, Waltham, MA) using $Cu_2O$ seeded Potassium Bromide (KBr) powder. UV-Vis spectroscopic measurement of absorbance spectra for $Cu_2O$ nanoparticles was performed using a (Shimatzu 1650PC) UV-Vis spectrophotometer. The $Cu_2O$ nanoparticles were dispersed in double distilled water, sonicated for 10 min and then their UV-VIS absorption spectra were recorded. The colloidal dispersions of $Cu_2O$ nanoparticles were kept in sample bottles for two months duration and the ageing effect was monitored with a frequency of 1 month on the basis of intensity variation of UV-VIS absorbance spectra.
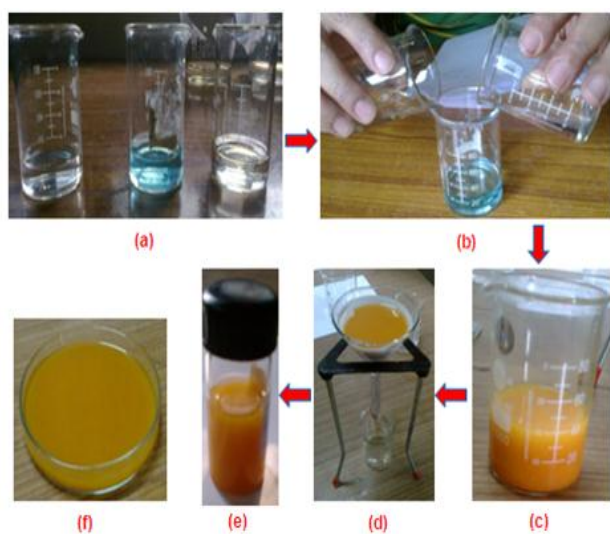


**Fig. 1** – Photographic illustration of steps involved in $Cu_2O$ nanoparticles synthesis (a) Solutions in beakers contain from left to right Ascorbic Acid, Copper Sulphate + PVP, Sodium Hydroxide.(b) Simultaneous addition (c) Precipitate of $Cu_2O$ nanoparticles (d) Filtration and washing (e) Colloidal dispersion of $Cu_2O$ nanoparticles (f) $Cu_2O$ nanoparticles in powder form

## 3. RESULTS AND DISCUSSIONS

### 3.1 Structural and Morphological Studies

Fig. 2 shows the XRD patterns of $Cu_2O$ nanoparticles with different ageing period such as (a) as synthesized, (b) 1 month ageing and (c) 2 months ageing. The XRD pattern (a) reveals the formation of single phase nanocrystalline cubic structure of $Cu_2O$ nanoparticles [JCPDS Card No 05-0667, $a = 4.2696$ Å (lattice constant value)]. The lattice constant ($a$) was calculated using the formula $a = d\sqrt{h^2 + k^2 + l^2}$ where $d$ is inter-planer distance and ($hkl$) are Miller indices. The calculated average value of lattice constant from XRD graph is $a = 4.2686$ Å and is in good agreement with standard value. No impurity phase was observed. The $2\theta$ values for prominent peaks, corresponding ($hkl$) planes and inter-planar distance ($d$) are represented in Table 1. The average crystallite size ($D$) in Å, was calculated by using Scherer's formula [18] given by (1)

$$D = \frac{K\lambda}{\beta\cos\theta} \tag{1}$$

where $K$ is the shape factor usually has a value 0.9, $\lambda$ is the X-ray wavelength and $\theta$ the Bragg angle and $\beta$ gives the full width of the half maxima (FWHM). The determined average crystallite size was 20 nm. The data represented in Table 1 match well with standard data for cubic phase of $Cu_2O$ as per JCPDS card. This has confirmed the formation of nanocrystalline, single phase $Cu_2O$ nanoparticles with cubical morphology.
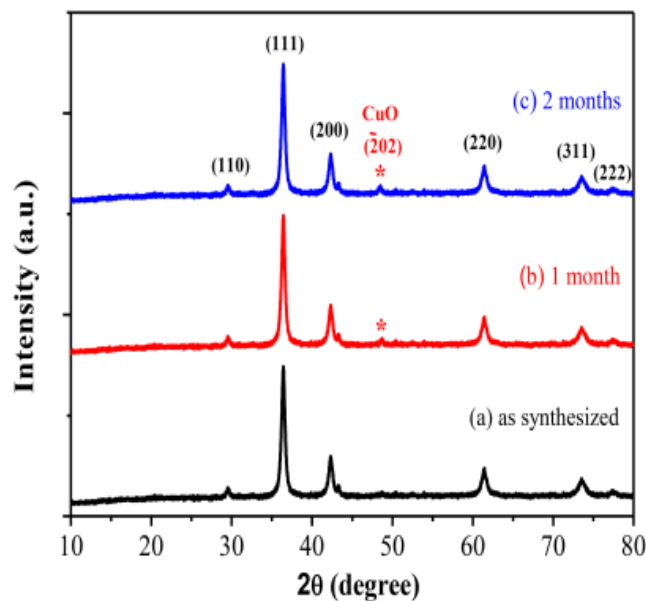


Fig. 2 – XRD patterns of $Cu_2O$ nanoparticles (a) as synthesized (b) 1 month ageing and (c) 2 months ageing

Moreover, XRD patterns in Fig. 2 (b) and (c) also shows the prominent $Cu_2O$ phase almost similar to Fig. 2 (a) with tiny traces of CuO phase indicated by a (202) peak at $2\theta$ value 48.52°. This shows that due to ageing a tiny amount $Cu_2O$ undergoes of phase change to CuO phase. The average crystallite size was also found to decrease to 19 nm and 16 nm due to ageing effect ageing period of 1 and 2 months.

**Table 1** – XRD analysis of $Cu_2O$ Nanoparticles (a) as synthesized

| $2\theta$ | ($hkl$) plane | Inter-planar distance ($d$) in Å |
|---|---|---|
| 29.6° | 110 | 3.012 |
| 36.4° | 111 | 2.464 |
| 42.2° | 200 | 2.136 |
| 61.3° | 220 | 1.510 |
| 73.4° | 311 | 1.287 |
| 77.4° | 222 | 1.232 |

SEM micrograph of as synthesized $Cu_2O$ nanoparticles is shown in Fig. 3 It shows that the room temperature synthesis in the presence of surfactant (PVP) the $Cu_2O$ nano-cube growth becomes selective along {111} direction and is truncated along {100} direction. Such a $Cu_2O$ nano-cubes are very stable from energy point of view because the specific surface area across the corners of nano-cubes is larger which enhances corrosion rate in the presence of PVP [19]. Further; through its

selective adsorption on $Cu_2O$ surfaces, PVP had reduced the growth rates of some of the faces of $Cu_2O$ and thereby effected for highly anisotropic growth of $Cu_2O$ nanocubes [20]. Hence, the growth rate along the direction of crystallographic plane {100} was greatly reduced on the other hand it was greatly enhanced along {111} plane. Thus; PVP the capping agent, has kinetically controlled the growth $Cu_2O$ nanocubes. The estimated average edge length of $Cu_2O$ nanocubes was $20 \pm 5$ nm which is in good agreement with XRD data.
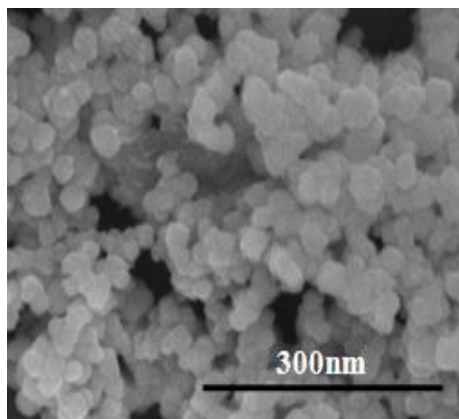


**Fig. 3** – SEM micrograph of $Cu_2O$ nanoparticles

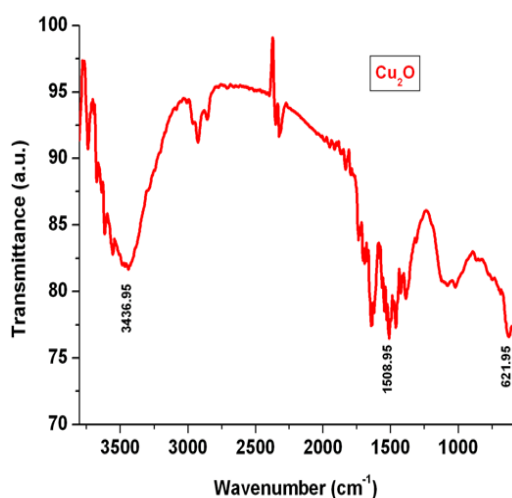The presence of characteristic functional group of $Cu_2O$ in the sample is revealed with FTIR as shown in Fig. 4.



**Fig. 4** – FTIR spectrum of $Cu_2O$ nanoparticles

A wide band centered at $3436.95$ cm$^{-1}$ was ascribed to H–OH stretching, while the band centered at $1508$ cm$^{-1}$ was assigned to H–OH bending. Further, the characteristic band centered at $621.95$ cm$^{-1}$ for $Cu_2O$ was ascribed to the vibrational mode of Cu–O in $Cu_2O$ phase [21]. Therefore, this has confirmed the formation of $Cu_2O$ nanoparticles.

### 3.2 Optical Properties

UV-VIS absorption spectra of $Cu_2O$ nanoparticles with different ageing period such as (a) as synthesized, (b) 1 month ageing and (c) 2 months ageing are represented.
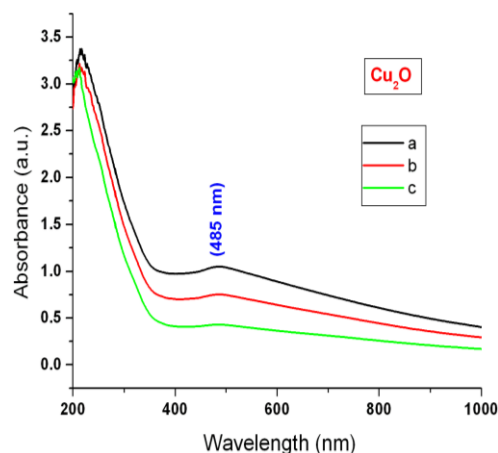


**Fig. 5** – UV-VIS absorption spectra of $Cu_2O$ nanoparticles recorded (a) as synthesized (b) after one month (c) two months of $Cu_2O$ nanoparticles

Besides, the location of the characteristic absorption peak was observed at the same position when absorbance spectra was taken (a) immediately when $Cu_2O$ nanoparticles were formed and (b) even again after a span of one month and (c) two months without any additional absorption peak has substantiated the stability of $Cu_2O$ nanoparticles.

The optical bandgap ($E_g$) of the as synthesized $Cu_2O$ nanoparticles was calculated using the Tauc relation [24] given by (2).

$$\alpha h\nu = (h\nu - E_g)^n \qquad (2)$$

Here, $\alpha$ is an absorption coefficient, h is Planck constant, v is the frequency and hv is the incident photon energy whereas $n$ is the exponent that determines the type of electronic transition causing the absorption and can take the values 1/2, 2/3, 2 and 3/2. The best linear relationship is obtained by plotting $(\alpha h\nu)^{1/2}$ against hv, indicating that the optical bandgap due to a direct allowed transition i.e for direct band gap semiconductor. Fig. 6 represents the plot of $(\alpha h\nu)^{1/2}$ vs hv for $Cu_2O$ nanoparticles. The direct band gap ($E_g$) of our sample was measured from the absorption coefficient data as a function of wavelength using Tauc relation thereby extrapolating the straight line of the $(\alpha h\nu)^{1/2}$ vs. $h\nu$ plot to intercept on the horizontal photon energy axis and was found to vary from 2.7 eV to 2.8 eV as shown in Fig. 6 for the same (a) (b) (c) samples mentioned above. These $E_g$ values are higher than the theoretical direct bandgap (2.2 eV – bulk $Cu_2O$) mainly due to nano size which leads to quantum confinement effects [1-6]. This is further confirmed from the increase in bandgap values for $Cu_2O$ nanoparticles with aging time mainly due to decrease in particle size and internal stress due to selective etching/corrosion leading to anisotropy. This is quite interesting and can be attributed to the quantum confinement effect in the nanometer regime on account of reduction of the particle size and can be visualized through blue shift.
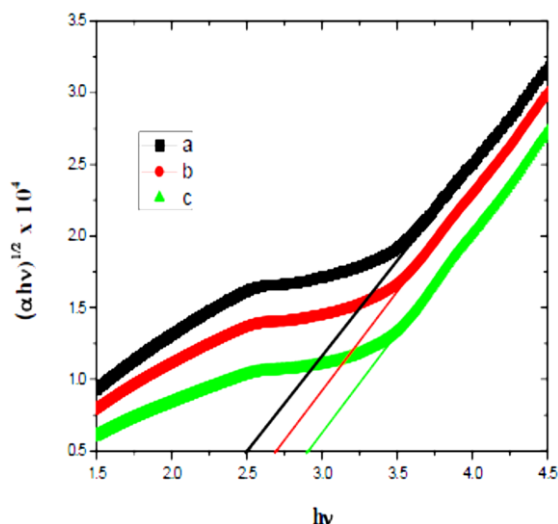
**Fig. 6** – The plot of $(\alpha h\nu)^{1/2}$ vs hv for $Cu_2O$ nanoparticles to monitor the aging effect on the band gap value for the samples taken after (a) just formed (b) one month (c) two months

## 4. CONCLUSIONS

The $Cu_2O$ nanoparticles were successfully synthe-

sized with a novel, facile, room temperature method. XRD and SEM results showed that the synthesized $Cu_2O$ nanoparticles were single phase, uniform, monodispersed and crystalline with cubical morphology. The average size i.e. edge length of nanocubes was 20 nm. FTIR also confirmed the presence of characteristic functional group of $Cu_2O$. UV-VIS absorbance spectra taken over the period of time of two months has substantiated its phase stability. The study has also revealed that the ageing causes tiny amount of $Cu_2O$ to undergo the phase change to form CuO thereby reducing the particle size of $Cu_2O$ leading to increase in the energy bandgap values owing to quantum size effect. Further, the demonstrated synthesis method is one pot, solution phase, and template free and economical. It is repeatable and easy to scale up.

## REFERENCES

1.  R. Toth, R. Kilkson, D. Trivich, *J. Appl. Phys.* **31**, 1117 (1960).
2.  A. Young, C. Schwartz, *J. Phys. Chem. Solid.* **30** No 2, 249 *(*1969).
3.  R. Kuzel, F. Weichman, *J. Appl. Phys.* **41** No 1, 271 (1970).
4.  Berezin, F. Weichman, *Solid State Commun.* **37** No 2, 157 (1981).
5.  I. Grozdanov, *Mater. Lett.* **19** No 5-6, 281 (1994).
6.  M. Shen, T. Yokouchi, S. Koyama, T. Goto, *Phys. Rev. B* **56** No 20, 13066 (1997).
7.  Y. Liu, H. Turley, J. Tumbleston, E. Samulski, R. Lopez, *Appl. Phys. Lett.* **98** No 16, 162105 (2011).
8.  M. Hara, T. Kondo, M. Komoda, S. Ikeda, K. Shinohara, A. Tanaka, J. Kondo, K. Domen, *Chem. Commun.* **3**, 357 (1998).
9.  P. Poizot, S. Laruelle, S. Grugeon, L. Dupont, J. Taracon, *Nature* **407**, 496 (2000).
10. J. Zhang, J. Liu, Q. Peng, X. Wang, Y. Li, *Chem. Mater.* **18** No 4, 867 (2006).
11. J.D. Snoke, *Science* **273** No 5280, 1351 (1996).
12. Y. Luo, Y. Tua, Q. Renb, X. Daia, L. Xingb, J. Lib, *J. Solid State Chem.* **182** No 1, 182 (2009).
13. H. Xu, W. Wang, W. Zhu, *Microporous Mesoporous Mater.* **95** No 1-3, 321 (2006).
14. Y. Yua, F. Dua, J. Yuc, Y. Zhuangd, P. Wong, *J. Solid State Chem.* **177** No 12, 4640 (2004).
15. L. Huang, F. Peng, H. Yu, H. Wang, *Mater. Res. Bull.* **43** No 11, 3047 (2008).
16. H. Shin, J. Song, J. Yua, *Mater. Lett.* **63** No 3-4, 397 (2009).
17. Y. Sui, Y. Zeng, W. Zheng, B. Liu, B. Zou, H. Yang, *Sens. Actuat. B* **171-172**, 135 (2012).
18. H. Klug, L. Alexander, *X-Ray Diffraction Procedures: For Polycrystalline and Amorphous Materials* (New York, USA: John Wiley and Sons: 1974).
19. Y. Bai, T. Yang, Q. Gu, G. Cheng, R. Zheng, *Powder Technol.* **227**, 35 (2012).
20. H. Zhang, Z. Cui, *Mater. Res. Bull.* **43** No 6, 1583 (2008).
21. E. Heltemes, *Phys. Rev.* **141**, 803 (1966).
22. L. Gou, C. Murphy, *J. Mater. Chem.* **14** No 7, 735 (2004).
23. L. Gau, C. Murphy, *Nano Lett.* **3** No 2, 231 (2003).
24. R. Swarnkar, S. Singh, R. Gopal, *Bull. Mater. Sci.* **34** No 7, 1363 (2011).